Remote Instrumentation Science Environment for Intelligent Image Analytics

Mauro Lemus Alarcon*, Songjie Wang*, Nguyen Nguyen†, Ashish Pandey†, Filiz Bunyak*,
Matthew Maschmann*, Kannappan Palaniappan*, Prasad Calyam*
*† University of Missouri - Columbia, USA.
Email: *{lemusm, wangso, bunyak, maschmannm, pal, calyamp}@missouri.edu; †{npntz3, apfd6}@mail.missouri.edu

2022 IEEE 18th International Conference on e-Science (e-Science) | 978-1-6654-6124-5/22/$31.00 ©2022 IEEE | DOI: 10.1109/ESCIENCE55777.2022.00023

***Abstract*—Current scientific experiments frequently involve control of specialized instruments (e.g., scanning electron microscopes), image data collection from those instruments, and transfer of the data for processing at simulation centers. This process requires a "human-in-the-loop" to perform those tasks manually, which besides requiring a lot of effort and time, could lead to inconsistencies or errors. Thus, it is essential to have an automated system capable of performing remote instrumentation to intelligently control and collect data from the scientific instruments. In this paper, we propose a Remote Instrumentation Science Environment (RISE) for intelligent image analytics that provides the infrastructure to securely capture images, determine process parameters via machine learning, and provide experimental control actions via automation, under the premise of "human-on-the-loop". The machine learning in RISE aids an iterative discovery process to assist researchers to tune instrument settings to improve the outcomes of experiments. Driven by two scientific use cases of image analytics pipelines, one in material science, and another in biomedical science, we show how RISE automation leverages a cutting-edge integration of cloud computing, on-premise HPC cluster, and a Python programming interface available on a microscope. Using web services, we implement RISE to perform automated image data collection/analysis guided by an intelligent agent to provide real-time feedback control of the microscope using the image analytics outputs. Our evaluation results show the benefits of RISE for researchers to obtain higher image analytics accuracy, save precious time in manually controlling the microscopes, while reducing errors in operating the instruments.**

***Index Terms*—remote instrumentation, image analytics, intelligent agents, control feedback, collaboration workspaces**

I. Introduction

Many scientific workflows (e.g., development of new materials, biomedical research) involve the collection of large amount of imaging data from specialized instruments (e.g., high resolution microscopes such as scanning electron microscopes (SEM)), and subsequent transfer of these data to simulation centers for extensive analysis [1]–[4]. This process requires appropriate settings of instruments, large storage capabilities, high bandwidth network capability and security measures to transfer the collected data, and perform data transformations. Further, it involves setting-up of image analytics workspaces for multiple researchers to collaborate for sharing the data and results [5].

This material is based upon work supported by the National Science Foundation under Award Number: CMMI-2026847. Any opinions, findings, and conclusions or recommendations expressed in this publication are those of the author(s) and do not necessarily reflect the views of the National Science Foundation.

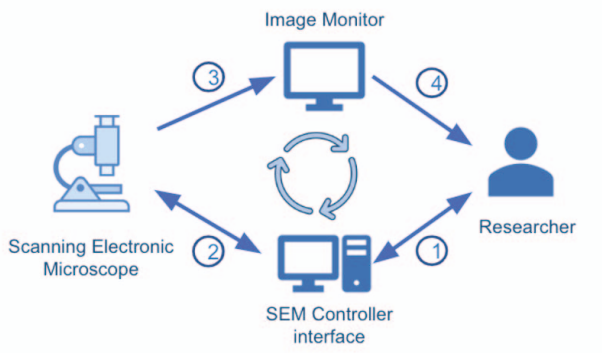

Fig. 1: Overview of scanning electron microscope experiment control process for image analytics.

The common setups of imaging instrument related workflows involve the execution of manual tasks across all points of the data pipeline. For example, as shown in Figure 1, first researchers need to prepare and setup experimental samples to be imaged on microscopes. Then researchers use controller interfaces to set up microscope imaging parameters, such as field of view (FoV), resolution, contrast, depth, image format (.TIF, .GIF, or .JPEG) [1], [2], and volume information (if 3D reconstruction needed) [3], [4] to collect image/volume data. For microscopes such as SEM, there are also microscope-specific meta settings such as temperature, chamber pressure, and accelerating voltage [6], [7]. The data collected from these microscopes will include both the microscope setting data, imaging parameters data, and the images/volumes themselves. During this process, the researcher will need to continously monitor the image/volume quality, and adjust the microscope settings and imaging parameters. The high reliance of manual intervention for image monitoring could introduce errors, increase the workflows processing time, which in turn affects the efficiency of valuable/expensive instrumentation resources usage and the effectiveness on producing timely results.

This work is motivated by two scientific research workflows, i.e., material properties discovery of carbon nanotube (CNT) growth process in SEM [1], [2], [8], and biological properties discovery of mitochondrial segmentation process in Electron Microscopy (EM) image volumes [9], [10]. These two research workflows involve collection of large number of

978-1-6654-6124-5/22/$31.00 ©2022 IEEE
DOI 10.1109/eScience55777.2022.00023

images/volumes using SEM, and subsequent machine learning/deep learning analysis of the collected images to guide researchers to either adjust experimental parameters to optimize CNT growth, or identify critical pathological indicators for identification of potential diseases. In both cases, due to the computing- and storage-intensive nature of the workflows, it is nearly impossible for researchers to know if the image volumes taken are satisfactory while they are in the imaging process. Thus, it is critical that the imaging and analysis processes are iteratively automated, so the researchers can get real-time feedback from the analysis results and use the feedback to help optimize experimental parameters. However, currently available cloud-based solutions typically solve a sub-problem in instrument-based scientific workflows, e.g., providing remote access to microscopes [5], or enhancing workflow analysis by improving machine learning/deep learning frameworks/algorithms [10], [11]. They are not capable of automating the entire workflow using AI/ML to leverage the analytics outputs and provide real-time guidance to the researchers to: (a) help them adjust the settings on the microscopes, or (b) optimize the parameters of image/volumes during microscope imaging process, to save both researcher's time and valuable microscope resource usage.

In this paper, we propose a Remote Instrumentation Science Environment (RISE) for intelligent image analytics that addresses the aforementioned difficulties in real-time imaging and data analytics workflows. RISE provides the infrastructure to securely capture images, determine process parameters and provides experimental control actions via automation, under the premise of "human-on-the-loop", where researchers can monitor all steps of the process, and adjust the instrument settings by following the recommendations of the analytic models. RISE supports collection of data generated from imaging instruments (e.g., SEM) and uploads it to a cloud-based storage repository, where AI/ML models can analyze and characterize the collected images. The characterization results are stored in a knowledge base that can be used by another intelligent agent to provide feedback on instrument settings to refine the results in the next iteration. Thus, researchers can use RISE to monitor the imaging process and tune instrument settings as needed.

To prove the effectiveness of this approach, we implement and evaluate our RISE in the two aforementioned research workflows by leveraging reinforcement learning (RL) based CNT growth analytics, and deep neural network (DNN) based mitochondria instance segmentation. Using RISE, we show how intelligent agents can utilize the characterization generated by AI/ML models to recommend pertinent control feedback to the microscope to improve the results in the next iteration of the process.

The remainder of this paper is organized as follow: Section II presents related work. Section III describes the RISE requirements for each use case. Section IV details the RISE implementation. Section V presents RISE performance evaluation. Section VI concludes this paper.

II. Related Work

A. Cloud-based Remote Instrumentation

Increased access to high-speed networks and growing data resolutions has made remote access of sophisticated scientific instruments such as microscopes and spectrometers widely feasible and essential for domain scientists in areas such as biochemistry, and material science/engineering. Important works have been proposed to automate RI-based processes. An edge-cloud microservice infrastructure named BRACELET was proposed in [12]. BRACELET focuses on edge-cloud infrastructure, incorporating new and old devices to create the BRACELET system to enable integration of cloudlets into an existing two-tier cloud-based infrastructure. This edge-cloud infrastructure helps to address the performance and security challenges that old scientific instruments face when they are connected to the cloud through a public network.

Multiple factors such as network bandwidth and remote operation limitations could affect the users' quality of experience (QoE) when accessing scientific instrumentation remotely. A prior work in [5] proposed a remote instrumentation and collaboration environment (RICE), which addressed some of the constraints by optimizing data transmission rates based on available network bandwidth, blocking users actions during extreme congestion situations to prevent system breakdown, and allow experts to control scientific instruments remotely. From a resource abstraction service perspective, authors in [13] proposed an instrumentation and measurement cloud (IMC) system, which focused on provisioning of traditional IM systems delivered on-demand, and with scalability. IMC enables remote sharing of IM resources, increased utilization of various resources, and facilitates processing and analysis of large volumes of data from instruments and sensors.

Increased remote usage of imaging instruments through cloud and networks also put them under serious security risks in e.g., data acquisition, data analytics and data collaboration processes. In [14], the authors used the STRIDE model, and analyzed the security threats to electron microscopy workflows' life cycle stages. The threat model addressed data acquisition, analysis and collaboration life cycle stages pertaining to e.g., materials modeling or biological specimen analysis that generate large amounts of raw and processed data sets and image files. To address these security issues, authors then proposed resource formalization, alignment, and allocation methodologies for securing data-intensive applications on multi-cloud infrastructure.

Although the above works provide important advances to increase accessibility to instruments from remote sites and enable sharing of data resources among collaborators, they do not integrate AI/ML models on cloud-based workspaces for instruments. Network-level security and related web services also have been under-studied for such RI collaboration environments. In contrast to prior work, our proposed RISE provides researchers a secure and cloud-integrated access to AI/ML models to obtain real-time feedback and increase efficiency in sharing image analytics results. In addition, our

intelligent agent-based feedback control mechanism allows researchers to setup automated interactions with microscope instruments on-the-fly. This enables researchers to adjust experiment settings and achieve efficient workflows that are automated to increase consistency and reduce errors.

B. Real-time Image Analysis and Instrument Control Feedback

Research in [15] proposed a data acquisition and analysis framework named "4CeeD" for cyber-physical environments in the material science domain. This framework focuses on the potential of capturing, accurately curating, correlating, and coordinating materials-to-devices digital data in a real-time manner. It also ensures these steps happen in a trusted manner before fully archiving and publishing them for wide access and sharing.

In [16], authors present Smartscope, a semi-automation framework to simplify and automate the screening process of cryoEM grids. This framework abstracts the intermediate steps of specimen navigation, then saves metadata into a database and presents the results to the user through an interactive web interface. Substrate from images are automatically detected and labeled using neural network-based approaches. The analysis results are then used to guide microscopists/researchers to visualize the specimen at increasing magnifications by navigating to areas that are most likely to provide information useful to guide the optimization.

Authors in [17] proposed an artificial intelligence atomic force microscope (AI-AFM) that is capable of not only pattern recognition and feature identification in ferroelectric materials and electrochemical systems, but can also respond to classification via adaptive experimentation with additional probing at critical domain walls and grain boundaries. By using a machine learning strategy, this framework makes real-time classification and control possible during scanning of materials under a microscope, and reduces the need of human insight on execution and image analytics, which are often tedious.

In [18], authors showed the importance of having real-time control feedback for microscopes. A desktop-computer based application was developed to fulfill those needs. Using real-time feedback control, they significantly simplified access to hardware, coding for remote control, and minimized the resources and manual efforts. Similarly, work in [19] presented a crystallization monitoring unit consisting of an in-situ digital microscope and real-time image analytics for monitoring and control of a micron-sized, liquid-liquid crystallization of calcium carbonate.

The authors in [20] designed an image analytics based direct nucleation control (IA-DNC) process, which is a model free feedback control strategy for batch and continuous crystallization processes. In this method, microscopy images are captured and processed by means of image analytics in real time and then feedback is provided to the microscope to further analyze and monitor the crystallization processes to ultimately achieve a stable and converged control of crystal shape.

While above works tried to address remote instrumentation needs and issues in the contexts of image analytics and data collaboration, none of these works utilized intelligent agent based approaches to offer recommendations to help researchers to make the right instrument parameter settings during their experiments. In our approach, intelligent agents are used to orchestrate main aspects of the remote instrumentation process elements such as remote operation, AI/ML model based feedback control to imaging instruments, data security concerns, and automation of the entire pipeline with minimized human-in-the-loop considerations. More importantly, our proposed intelligent agent approach fully integrates both the web portal and back-end machine learning/deep learning models for data analysis. It leverages a knowledge base to provide interactive recommendations in real-time to help researchers control the instruments to obtain the desired experiment settings, thus saving precious time of researchers/instruments, and maximizing workflow outputs.

III. Research Use Case Requirements

In this section, we present the two research uses cases whose workflow process automation delineate the architectural requirements of the RISE design and implementation.

A. Carbon Nanotube Growth Automation Use Case

1) Research Background

Carbon nanotubes (CNTs) are widely studied for their promising mechanical, electrical, and thermal properties that make them suitable for diverse applications [1]. When CNTs are synthesized in dense populations known as CNT forests, a significant performance gap between individual CNTs and CNT forests is observed, as shown in Figure 2. To date, overcoming the performance gaps has not been achieved due to a lack of understanding about how the processing mechanisms of CNT synthesis control the CNT self-assembly process [11].

It is extremely difficult to obtain a desired property set from a CNT growth in forests. CNT growth involves a large set of parameters, making experimental and/or numerical exploration of the synthesis prohibitive. The CNT synthesis parameters include e.g., catalyst composition, thickness, CNT synthesis temperature, gas composition, pressure, synthesis time, and more. In real experiments, researchers often utilize CNT forest simulation to guide CNT forest synthesis experiments. For example, a time-resolved finite element method (FEM) CNT forest simulation tool [1], [21] is used as a high-throughput virtual laboratory to examine the synthesis–structure–property design loop of CNT forests. Images of each CNT forest morphology are obtained at the end of their simulated synthesis, and a mechanical compression simulation is performed to obtain mechanical properties [21]–[23]. Numerical simulation of CNT forests synthesis and self-assembly is an alternative approach that may increase the speed and diversity of synthesis parameters examined. Such simulations can predict both the CNT forest structural morphology and the resulting CNT forest properties. By systematically varying CNT synthesis parameters, one may arrive at a set of conditions that produce the desired CNT forest performance metrics such as mechanical stiffness and thermal conductivity.

In CNT research efforts, experimental results are hard to obtain, and they are usually noisy, expensive and time consuming. The CNT forest attributes (CNT diameter, areal density, growth rate) are poorly characterized and time variant. Therefore, the physics-based simulation of CNT forests may present a reliable and powerful tool for training ML models in the absence of suitable experimental data, and can be used with experimental data collaboratively to provide more accurate control of CNT growth experiments.

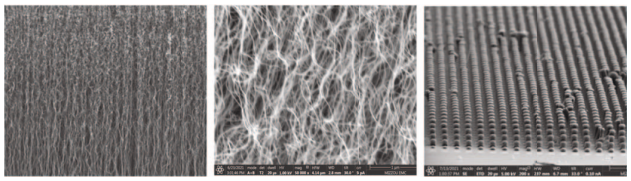

Fig. 2: SEM images of CNT forest with three different morphology each potentially having different mechanical properties: (left) tortuous morphology, (middle) well-aligned morphology, and (right) patterned growth using photolithography.

2) CNT Growth Experiment Workflow

Multiple factors that contribute to the growth and final result of carbon nanotube (CNT) forest, and in-situ CNT growth experiments require long preparation time and active human intervention to regulate the synthesis parameters in search of specific material characteristics. Implementing the CNT growth process in a system able to regulate the parameters, without human intervention in real-time based on in-situ imagery, would facilitate the study of CNT forest synthesis and self assembly to deterministically achieve prescribed material properties.

To elucidate the process-structure-property relationships of carbon nanotube (CNT) forests, our approach will use AI/ML models to conduct iterative physical and numerical synthesis experiments, characterize the results, learn from the results, and then alter the experimental conditions to converge upon a user-defined CNT forest property set. The ultimate goal is to perform the process without human interaction, so the process control will shift from a human user to an autonomous system.

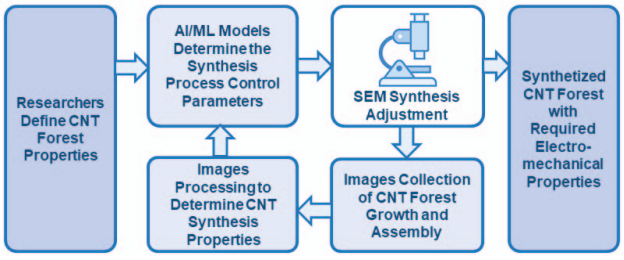

Fig. 3: CNT Growth Automation Process including the AI-based model that determines and sets the synthesis process control parameters, the SEM where the CNT process takes place, and the images collection and analysis to determine the CNT properties.

As illustrated in Figure 3, the CNT growth automation process involves the following steps: 1) in-situ scanning electron microscope (SEM) synthesis techniques to acquire imagery of CNT forest growth and self-assembly, 2) computer vision to quantify and isolate the kinetics and assembly mechanisms of CNTs, 3) a complimentary finite element CNT forest synthesis and testing simulation, 4) a convolutional neural network (CNN) to predict CNT forest properties from experimental and simulated images, and 5)a distributed control algorithm that will transition experimental manual control from human researchers to a "human-on-the-loop" control assisted by autonomous decision algorithms. As the CNT growth kinetics and self-assembly process are understood for diverse synthesis conditions, the CNN will predict the process-structure-property relationships for CNT forests.

3) Workflow Automation Requirement

Human action and observation are often biased and tend towards guesswork when determining simulation or experimental synthesis parameters, especially when iteratively navigating multi-dimensional parameter spaces. This can result in user actions and materials discovery progressing in either stable (i.e., processing steps produce predicted material responses), unstable (i.e., processing steps produce undesired responses) or breakdown (i.e., processing steps provide no material response) states. To understand and map the process-structure-property relationships for CNT forests, there is a need for remote control and an iterative experimentation approach with integrated analysis, simulation, and feedback mechanisms to gradually remove humans, with their inherent error and bias, from the CNT property discovery loop. This will include obtaining the CNT growth experimental settings, the parameters for image taking, real-time analytics of image data, and using the analytics output as guidance to control experimental settings on-the-fly to improve CNT growth quality. To this end, our proposed control feedback mechanisms help characterize and guide physical processes through on-the-fly deep learning algorithms and an intelligent chatbot agent that provides semi- and fully-automated guidance in CNT synthesis.

B. Mitochondria Segmentation Automation Use Case

1) Research Background

Mitochondria are membrane bound organelles that play key roles in cellular energy production, calcium homeostasis regulation, free radical production, steroid synthesis, and cell death [24]. Evidence suggests that mitochondria can be associated with mechanisms involved in aging, neurodegenerative diseases, cancer, and metabolic disorders [24]–[27]. Scientists rely on EM to study morphology of subcellular structures like mitochondria. The first step towards characterization of mitochondria morphology is image segmentation that aims to identify mitochondrial regions from the rest of the input image. Given density and complexity of mitochondrial structures in the imaged biological samples, and the size of the image data (hundreds of slices per sample), manual segmentation of mitochondria is a labor-intensive and subjective task.

Automated image processing techniques are needed to segment, quantify, and analyze the large volumes of EM image data. Various methods and pipelines have been proposed for mitochondria segmentation [28], particularly owing to

the recent advances in deep learning [29], [30]. Our related advances are in EM image analytics in general [3], [31] and mitochondria segmentation in particular [9], [10]. An example diagram showing the mitochondria segmentation validation analysis in a human tissue sample is shown in Figure 4.

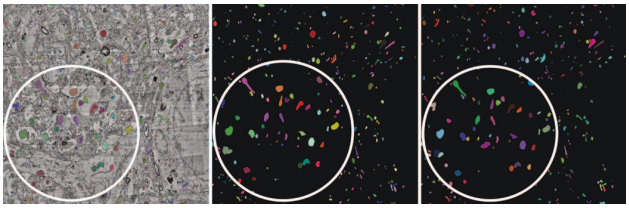

Fig. 4: Instance segmentation results in an image slice of a human validation dataset. Sample result is illustrated on a single slice (middle). Colored overlays correspond to mitochondrial regions (left), and the label ground truth (right).

2) Mitochondria Segmentation Experiment Workflow

The mitochondria image segmentation process aims to identify mitochondrial regions in EM images. The process also involves detection of mitochondrial boundaries in order to help separate neighboring mitochondria to allow individualized characterization. Due to imaging and sample complexities, microscope parameters need to be adjusted to improve image characteristics and outcomes during the data analysis process. Current workflow processes rely on in-situ researchers for instrument setting adjustments, data collection and transmission to simulation centers. Once data is analyzed, a request for new data is submitted indicating the adjustments needed to improve the characteristics of the images. Given the involvement of the human effort on the process, it requires a long time to complete the process with the expected outcomes. Implementing a mitochondria segmentation process in a system allows adjustment of the microscope parameters, without human intervention in real-time based on in-situ imagery, which expedites the process and provides successful results faster.

Our mitochondria segmentation process uses a deep learning based pipeline which takes input image patches generated by electron microscopy. The processing pipeline consists of a 3D convolutional long short term memory U-Net (3D CLSTM U-Net) segmentation network followed by a marker-controlled watershed segmentation step for instance segmentation [10] as shown in Figure 5. We compute a number of mitochondria count, size, shape characterization and segmentation evaluation measures [32] to localize regions of interest and to assess segmentation quality. These parameters can be used by another AI-based model to generate a feedback command looking to improve the quality of the image and facilitate the analysis in order to foster better outcomes. In this way, the full process can be conducted with limited human interaction, where images are collected by a remotely operated SEM with commands generated as a feedback from the results of the mitochondria segmentation process.

This process will require the following steps: 1) in-situ scanning electron microscope (SEM) image collection from tissue sample, 2) data transmission to a cloud-based simulation

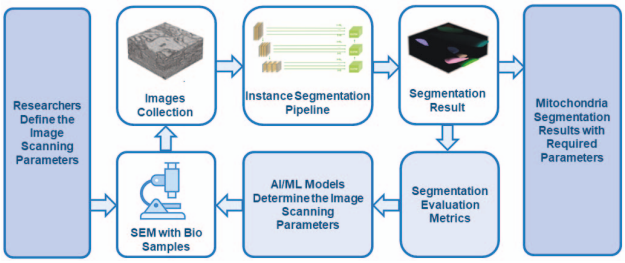

Fig. 5: Mitochondria segmentation pipeline. Experimental images of biomedical samples are taken and collected from multi-beam SEM. The images are then passed through instance segmentation pipeline, where machine learning algorithms are utilized to recognize and isolate mitochondria from the images/volumes. A set of unsupervised evaluation metrics are computed. The segmentation results in the form of mitochondria region and boundary maps are remapped back to the images, and matched to ground truth labels to generate the accuracy output, represented by dice score and average precision (AP) results. An AI-based model uses these results to set the SEM image scanning parameters.

center, 3) patch-level segmentation using a 3D convolutional network, 4) a full volume instance segmentation, 5) computation of various outcome measures including but not limited to mitochondria size, shape, density in a region, segmentation confidence values, unsupervised segmentation quality evaluation measures, 6) use a second AI-based model to process these outcome measures to generate a feedback command, 7) use the feedback command to adjust the microscope parameters.

3) Workflow Automation Requirement

Similar to the CNT growth use case, the mitochondria segmentation workflow is also time consuming, involving human-in-the-loop during image data collection, analysis and changing parameters on the microscope during sample imaging processes. In addition, biomedical samples are difficult to prepare if the current experiment fails and researchers have to spend a long time and a lot of efforts to repeat the same experiment. In this case, an automated workflow that involves image data import, data collection and accurate analysis, and a real-time feedback guidance with the analysis output results. These steps will benefit the researchers in their experiments by automatically assessing image data quality and adjusting microscope settings as well as imaging parameters.

IV. RISE System Implementation

In this section, we describe the architecture of the RISE system and its components. We also provide the description of the modules, the interfaces and their interactions.

A. System Architecture Overview

Based on the requirements described in the previous section, we defined the system architecture as depicted in Figure 6. It includes various modules, including the SEM controller agent, the Analytic Services Broker integrated by AI/ML models provided to analyze the images from the SEM, and to generate the feedback commands intended to adjust the SEM settings. A data repository and knowledge base component is intended to store the images collected from the SEM, and the results

generated from the AI/ML model and associated meta data for each image. A web portal provides the user interface for researchers and system administrators to interact with the system. Detailed descriptions about the specifications and implementation details of this RISE architecture are provided below.

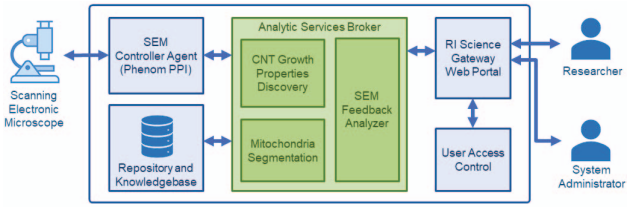

Fig. 6: RISE architecture featuring various modules, including an Analytic Services Broker, the SEM Controller Agent, the Web-based User Interface, User Access Control, Data Repository and Knowledge Base.

B. Web-based User Interface

The *Web-based User Interface* module includes a web portal, User Access Control functions and chatbot services that allow researchers and system administrators to interact with the RISE system. Through the web portal service, users can monitor the status of experiments, determine if images have been generated by the SEM, preview available images, submit images for analysis and get the related results from the analytic services, and share the images and results with other researchers as shown in Figure 7. The web-portal relies on the User Access Control module to allow users access to specific resources and functionality, and to limit, permit, or deny access from users, resources or locations. Using the chatbot service, researchers can get a set of recommendations about the update on parameters (i.e., image resolution, image size, move to specific scanning area) that can be applied on the SEM, based on the last experiment iteration results, and that are expected improve the outcome of the next experiment iteration. Researchers can select one option for each parameter and upon confirming the selection. The chatbot communicates the decision to the web portal engine, which translates it into the proper API command to be sent to the SEM Controller agent looking to set the SEM instrument parameters accordingly.

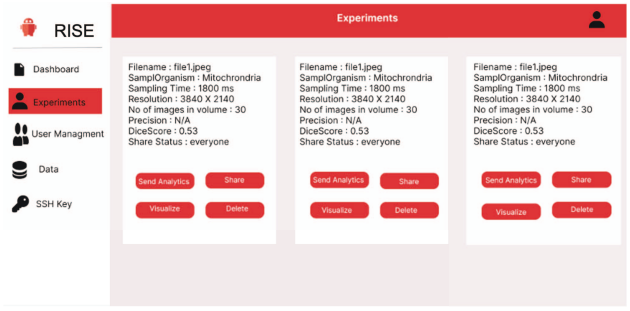

Fig. 7: RISE web portal interface displaying the information of the experiments from a user's account.

Our approach includes a chatbot intelligent agent that interacts with the researchers within the RISE system web portal as illustrated in Figure 8, and provides critical recommendations during feedback control of researcher's experiment. The chatbot agent is implemented using the Dialogflow API maintained by Google to promote human–computer interaction based on natural language conversations. The chatbot agent takes the results from the CNT growth model and the mitochondria segmentation model generated by the Analytic Services Broker, which helps to determine recommendations for researchers to make necessary adjustments on SEM settings to improve the outcome of the experiment.

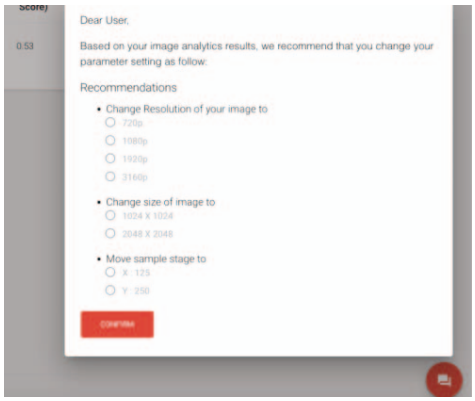

Fig. 8: RI Web Portal User Interface featuring the chatbot dialog showing the options researchers can select to refine the SEM settings.

C. SEM Controller Agent

The *SEM Controller Agent* is a module hosted at the location of the SEM. It works as the interface exposing the SEM resources to the Internet, and allowing the SEM to communicate with the other modules by receiving settings updates commands and providing scanned images and status information. This module is enabled to manage two API command sets. One API set handles the direct control of the SEM instrument by generating the commands to control its parameters, read the results of command actions, and monitor its status. The other API set handles the communication between the SEM controller agent and the web-based user portal interface, and works as a translator between the high-level commands sent by the web-portal and the SEM API commands. The SEM controller agent isolates the SEM instrument from any external environment, protecting it from any unauthorized access and related security risks. It encapsulates its proprietary API and wraps it into a high level API between the web-based user interface and the SEM controller agent. It also provides an open API that can be adapted to multiple SEM models, brands, technologies, and security requirements. Additional instruments can be added to the system just by including the agents with the proper API to control those instruments. Thus, a variety of instruments in the system can be made available for the researchers.

For implementation and testing purposes, we used a ThermoFisher Phenom desktop microscope. Consequently, our SEM Controller Agent was implemented using the Phenom Programming Interface (PPI) with the PyPhenom Library. The PPI methods implement the Phenom commands to get the instrument mode and operational mode, load/unload sample, perform sample navigation to specific area, update beam parameters; change the magnification, and adjust focus, brightness and contrast, and perform image acquisition.

D. Analytic Services Broker

The *Analytic Services Broker* includes the pre-trained AI/ML based models to discover the CNT growth properties and the mitochondria segmentation properties. This module interacts with the other modules to process the images collected from the SEM resources and provides the required feedback relating to adjustments that need to be applied on the SEM in preparation for the next experiment iteration.

For CNT use case, we used an AI-based model to characterize the images related to a CNT growth process. The model uses reinforcement learning (RL) [11] approach to learn from simulation-based images and characteristics of temporal CNT growth, and considering various growth parameters such as density, growth rate, tube radius, tube stiffness, and Van der Waals forces. The images generated by CNT growth process are analyzed by the RL agent to determine the waviness, i.e., deviation of the growing tubes from straight axial growth, and the average growth rate of the tubes. These results are then used to determine the proper settings that need to be sent to the SEM to adjust for getting the expected results in the upcoming iterations of the experiment.

The AI-based model associated with the mitochondria segmentation process uses a 3D deep convolutional network [10], which extends the classical U-Net semantic segmentation network with a convolutional long-short term memory (3D CLSTM U-NET). The images from SEM are analyzed by this model which generates two outputs, one corresponding to mitochondrial regions, and the other corresponds to mitochondrial boundaries. These region and boundary results are used by a watershed segmentation step for identification of individual mitochondria. The image analytics process also computes various outcome measures to quantify mitochondria density in a region, segmentation confidence values, and segmentation quality. These measures are used to determine the SEM parameters that need to be set to improve the outcome of the next image to be scanned by the SEM and to determine regions of interest to be imaged and analyzed in higher resolutions.

E. Data and Knowledge Base Repository

The collected images from the SEM resources, the metadata related to these images, the image processing results generated by the Analytic Services Broker, and the feedback commands compiled by the SEM Feedback Analyzer need to be stored. Our approach relies on a stable, secure, and open-standard SQL access repository to store, and manage all of this data. Besides applying the SQL standard approach, we define a centralized data repository featuring a *Common Data Model* repository (CDM) to store the raw images data, images related metadata, images related analytic results, and images related actions taken to influence subsequent experiment steps. Correspondingly, the CDM will contain the experiment ID, the raw image data, the related metadata, the image analytics results, action options advised, actions executed by the researcher, and obtained results. The richness of the information stored in the CDM could be leveraged by future works oriented to improve the results of the current experiments.

F. Risk Management in Scientific Workflow Control

Workflows setup is configured within an experiment definition via the web portal. The experiment definition contains the initial instrument setup, and the history of each iteration including instrument adjustments, results, and comments from the researcher. The information about the options provided by the Feedback Analyzer are also stored, as well as the option the researcher selected to generate the feedback command and adjust the instrument settings. Once an experiment iteration starts, the status of the instrument is continuously monitored by the SEM controller agent, and the latest status is reported to the web portal so that the researcher can follow the progress of the task. On the event of network failure or faulty component failure in the system, researchers can use the the historical information of the experiment to reestablish the the conditions of the last iteration and continue with the experiment, or completely recreate the process by using the instrument setup sequence applied on the iterations already completed. The AI recommendations on how to adjust the instrument for the next iteration can be verified by the researcher in the context of the "human-on-the-loop" approach. In this way, the researcher will have the opportunity to supersede the adjustments options provided by the feedback analyzer and adjust the instrument settings to progress the experiment in the desired direction.

V. Performance Evaluation

In this section, we describe our deployment of RISE system on a testbed, and evaluation of the system in both CNT and biomedical image analytics use cases.

A. RISE System Testbed Implementation

To evaluate the overall effectiveness and efficiency of our proposed RISE system, we implemented a testbed as shown in Figure 9 to deploy all the system components.

We used the University of Missouri (MU) Lewis HPC cluster to host the developed AI/ML models to analyze the images from the SEM. For both CNT growth process and mitochondria segmentation process, we deployed the AI/ML models as microservices that will constantly check for image/volume data inputs and will start to analyze the data once the inputs are received through API calls from the Web Portal, where data is sent from microscopes. Both models will store analysis outputs into the data repository and knowledge base, which is also deployed on the Lewis platform in the form

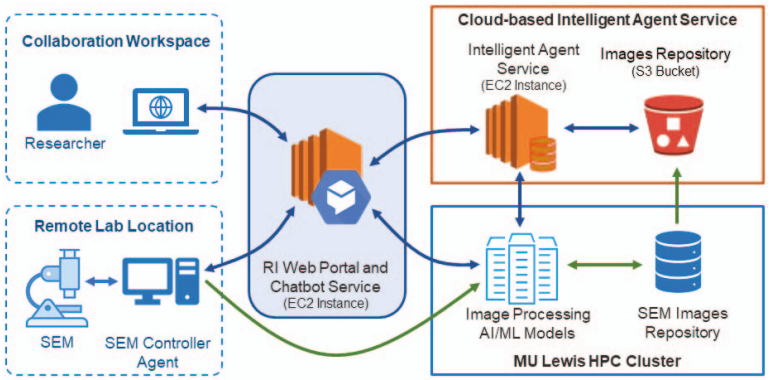

Fig. 9: RISE System testbed infrastructure showing workspace components including: the remote lab location of the SEM and the related controller agent with Internet access; the science gateway Analytic Services Broker with the images repository, image processing AI models and knowledge base, and web portal with the chatbot service.

of MySQL databases. The data repository is accessed by the SEM Controller Agent to store the scanned images from the SEM. It is also accessed by the cloud-based Intelligent Agent Service to retrieve images and metadata to define the SEM parameters to be set for the next iteration of the experiment. These SEM parameters will be used by the chatbot service to advise the researcher, and they are accessed by the Web Portal service to retrieve and display images and related metadata as requested by the researcher.

AWS was used to host the AI-based model and local images repository is used to determine the SEM settings to be applied based on the results generated by the SEM image analytics models. The public cloud deployment provides flexibility, scalability, and security standards. The Intelligent Agent Service accesses the SEM Images Repository in the HPC cluster and loads the required images into a local S3 Bucket repository for an immediate access to image data and metadata. The results of the analysis by this agent updates a local knowledge base that will be available for the chatbot service to advise the researcher on selecting the parameters to be set on the SEM to improve the outcomes of the next iteration of the experiment.

The Phenom SEM instrument is located in a MU research laboratory, managed by the Electron Microscope Core Facility, and allows access to the other modules of the system via the SEM Controller Agent implemented with the PPI interface. The agent isolates the instruments and translates the commands coming from the Web Portal into the proprietary instrument's API to setup the instruments and collect the scanned images. The scanned images are stored in the SEM Images Repository by the agent via a REST API.

B. CNT Use Case Experiments Results

The CNT growth experiment setup allowed researchers to evaluate the performance of the Q-learning based RL-models in their ability to regulate growth parameters to improve maximum compression load capacity of the CNTs. Given the long time taken by CNT growth processes and complexity of the experiment setup, we used simulated images [11] to expedite the images characterization, so CNT growth parameters (i.e., angular deviation, growth rate) can be used by the SEM feedback analyzer to generate the feedback commands intended to be used by an actual SEM.

1) Evaluation of model based on angular deviation

The Q-learning based RL agent was able to learn growth parameter temporally to create CNTs with ability to withstand more compressive forces. For this part of evaluation, we leverage the Q-learning framework previously developed by our team [11] using the "Wave" parameter. The "Wave" parameter controls rate of change of standard deviation of angle of growth for CNTs. The parameter ranges from 1 to 10, where 1 represents the smallest value and causes straight growth while 10 represents orthogonal growth. A larger value of the parameter signifies more waviness in tube growth at that growth step.

As shown in Table I, maximum compression load is observed at 90% of the maximum height of the CNT forest as densification occurs. Regardless, the maximum compression load of the system is improved at all the heights when the RL agent is used. We notice that the best configuration of growth is achieved for the [3,4,5] configuration of "wave" parameter. At all other growth parameters configurations, the maximum achieved compression load is less than the compression load achieved at [3,4,5] configuration.

TABLE I: Comparison of maximum load capacity of CNTs **based on angular deviations** at different heights, 'without' or 'with' our RL model; H represents the initial height of tubes before compression.

Height after Compression	Max. Load without model	Max. Load with RL model	Optimal "wave" Configuration
95% of H	01.43e-05	3.59e-05	[3,4,5]
90% of H	4.61e-05	6.43e-05	[4,4,5]
80% of H	2.1e-05	4.2e-05	[3,4,5]

2) Evaluation of model based on rate of growth

The RL model was able to learn the optimal growth rate variability to create CNT forests with increased yield forces. As shown in Table II, the average improvement in the load capacity increased by 183% at different heights of compres-

sion. The maximum improvement in compression load was 194%, which was noticed at 90% of compression at an average growth of 65 nm per step.

TABLE II: Comparison of maximum load capacity of CNTs **at different heights**, 'with' or 'without' our RL model. H represents the initial height of tubes before compression.

Height after Compression	Max. Load without model	Max. Load with RL model	Optimal Average Growth Rate
95% of H	2.56e-05	4.71e-05	65 e-9 m/sec
90% of H	3.58e-05	6.98e-05	65 e-9 m/sec
80% of H	2.81e-05	4.86e-05	60 e-9 m/sec

On comparing the results for maximum compression load within the two RL models as shown in Tables I and II, it can be noticed that the maximum load capacity in the model based on average rate of growth was better than the model based on change in standard angular deviation at all heights of compression. This could be because the standard deviation of angular deviation was fixed at 3 when model was trained with rate of growth parameter, which is very near to optimal configuration of [3,4,5] observed in model based on angular deviation. Regardless, the compression load capacity still improves when the model is trained with rate of growth or change in standard angular deviation as the base feature for model training.

The angular deviation, growth rate, and their correlation with the compression load capacity of the tubes as found by the validation of the RL-based agent are valuable parameters that the AI-based analyzer model in RISE can use to determine the proper feedback for the SEM. The feedback options provided can be used by the researcher on setting the SEM to control the CNT growth process.

C. Mitochondria Segmentation Experiment Results

The mitochondria segmentation experiment setup allowed researchers to evaluate the performance of the AI-based model in its ability to effectively identify and quantify mitochondrial structures in SEM imagery. Mitochondria density in a region, segmentation confidence values, and segmentation quality evaluation measures provided by this process are used as control parameters by the AI-based analytic model to generate the feedback commands intended to be used on the SEM.

1) Validation dataset and training model

The preliminary mitochondria instance segmentation experiments were conducted on the MitoEM dataset [4] collected by a multi-beam scanning electron microscope [33]. This dataset includes two stacked volumes. The first volume (Mito-H) contains 1000 2D image slices of size 4096×4096 acquired from an adult human cortex. The second volume (Mito-R) also contains 1000 2D slice images of size 4096×4096 captured from an adult rat cortex. Both of them have the same resolution of $8 \times 8 \times 30$ nm^3. The dataset was annotated by first using a 3D U-Net, and then corrected manually by experts [4]. In the experiment, each volume was split into training set (400 slices), validation set (100 slices), and test set (500 slices).

The 3D CLSTM U-Net was trained with random initialization. It used the Adam optimizer [34] with a learning rate of 0.0001 to minimize the binary cross-entropy loss function and dice loss function. For data augmentation, we applied a random xy axis flip with a probability of 0.5 and a random zoom with a scale from 0.8 to 1.25 and probability of 0.2. We perturbed the image intensity with random contrast with a probability of 0.2, Gaussian noise with a probability of 0.2, and Gaussian smoothing with a probability of 0.2.

TABLE III: Semantic segmentation performance of the proposed 3D CLSTM U-Net network.

Dataset	Region Dice	Boundary Dice
Mito-R	0.94	0.74
Mito-H	0.91	0.70

2) Experiment results

Our mitochondria segmentation performance is summarized in Table III in terms of dice score for semantic segmentation and in Table IV in terms of average precision (AP) scores with an intersection over union (IoU) threshold at 75% for instance segmentation. The high region dice scores of 0.94 and 0.91 in Table III for Mito-R and Mito-H respectively indicate that the proposed network is highly successful in segmenting mitochondrial structures from the rest of the image volume including other subcellular structures.

In Table IV the instance segmentation results are grouped based on the mitochondria size (small $\leq$ 5,000 voxels, medium 5,000 to 15,000 voxels, large $\geq$ 15,000 voxels). On average, the proposed 3D CLSTM U-Net network improves instance segmentation performance compared to regular 3D U-Net network [35] by 0.21 and 0.03 points for rat (Mito-R) and human (Mito-H) datasets respectively. These improvements are mostly due to improvements on large mitochondria. The lower performance on instance segmentation is mostly due to failure to separate touching mitochondria instances. Instance segmentation performance on the rat dataset is better compared to the human dataset because the rat dataset has a less denser distribution of mitochondria.

The proposed mitochondria segmentation network will be used by the RISE system for two primary purposes: (1) to perform a fast scan of the specimen in low resolutions in order to locate regions of interest containing mitochondrial structures to be further imaged and analyzed in higher resolutions; (2) to fine-tune imaging parameters such as focus to improve image quality and consequently analysis outcomes. The automated localization and region selection step will considerably reduce processing time associated with both imaging and image analysis. This will also help in reducing specimen degradation due to interactions with accelerated electrons during imaging. The parameter fine-tuning step will use the confidence scores obtained from the last layers of the segmentation network as an indicator for out-of-focus imaging or other non-optimal imaging parameters and guide selection of imaging parameters for improved outcomes.

TABLE IV: Instance segmentation performance in terms of average precision (AP) scores with an intersection over union (IoU) threshold at 75%.

Dataset	Method	Average	Large	Medium	Small
Mito-R	3D U-Net [35]	0.52	0.49	0.75	0.29
Mito-R	3D CLSTM U-Net	0.73	0.77	0.62	0.14
Mito-H	3D U-Net [35]	0.62	0.62	0.77	0.56
Mito-H	3D CLSTM U-Net	0.65	0.71	0.66	0.13

VI. Conclusion

In this paper, we introduced the architecture and implemented a RISE system that allows researchers to automate execution of workflows involving the collection of images from a scanning electronic microscope, and AI/ML model based image analysis to generate feedback for process control. The feedback is used to determine the parameters that can be used to control the next experiment iteration to avoid errors and improve efficiency of valuable/expensive scientific instrument resources. Motivated by a CNT growth workflow and a mitochondria segmentation workflow, we implemented RISE with intelligent agents to provide real-time feedback to intelligently update the instrument settings. From the CNT growth process we used the angular deviation of the tubes and its growth rate to determine a set of options that can be updated on the remote instrument to improve the compression load capacity of the tubes. From the mitochondria segmentation process, we used the dice score and average precision metrics as the parameters to generated the feedback control for the instrument to improve the quality of the scanned images. Thus, we showed that RISE system achieves an effective "human-on-the-loop" approach to automate scientific workflows, while improving consistency on images collection and increasing the results accuracy.

As part of our future work, we plan to expand the architecture to cover additional image analytics uses cases, increasing the parameters used by the intelligent agent to generate the feedback control of the instrument, refining the AI-based model and expanding the the feedback control options for the researchers to auto-control microscope settings.

References

[1] Taher Hajilounezhad, Damola M Ajiboye, and Matthew R Maschmann. Evaluating the forces generated during carbon nanotube forest growth and self-assembly. *Materialia*, 7:100371, 2019.

[2] Taher Hajilounezhad, Rina Bao, Kannappan Palaniappan, Filiz Bunyak, Prasad Calyam, and Matthew R Maschmann. Predicting carbon nanotube forest attributes and mechanical properties using simulated images and deep learning. *npj Computational Materials*, 7(1):1–11, 2021.

[3] Nguyen Phuoc Nguyen, Ilker Ersoy, Jacob Gotberg, Filiz Bunyak, and Tommi A White. Drpnet: automated particle picking in cryo-electron micrographs using deep regression. *BMC bioinformatics*, 22(1):1–28, 2021.

[4] Donglai Wei, Zudi Lin, Daniel Franco-Barranco, Nils Wendt, Xingyu Liu, Wenjie Yin, Xin Huang, Aarush Gupta, Won-Dong Jang, Xueying Wang, et al. Mitoem dataset: large-scale 3d mitochondria instance segmentation from em images. In *International Conference on Medical Image Computing and Computer-Assisted Intervention*, pages 66–76. Springer, 2020.

[5] Prasad Calyam, Abdul Kalash, Ramya Gopalan, Sowmya Gopalan, and Ashok Krishnamurthy. Rice: A reliable and efficient remote instrumentation collaboration environment. *Advances in Multimedia*, 2008, 2008.

[6] Azad Mohammed and Avin Abdullah. Scanning electron microscopy (sem): A review. In *Proceedings of the 2018 International Conference on Hydraulics and Pneumatics—HERVEX, Băile Govora, Romania*, pages 7–9, 2018.

[7] Kalsoom Akhtar, Shahid Ali Khan, Sher Bahadar Khan, and Abdullah M Asiri. Scanning electron microscopy: principle and applications in nanomaterials characterization. In *Handbook of materials characterization*, pages 113–145. Springer, 2018.

[8] Gordon Koerner, Ramakrishna Surya, Kannappan Palaniappan, Prasad Calyam, Filiz Bunyak, and Matthew R Maschmann. In-situ scanning electron microscope chemical vapor deposition as a platform for nanomanufacturing insights. In *ASME 2021 International Mechanical Engineering Congress and Exposition*. American Society of Mechanical Engineers Digital Collection.

[9] Ismail Oztel, Gozde Yolcu, Ilker Ersoy, Tommi White, and Filiz Bunyak. Mitochondria segmentation in electron microscopy volumes using deep convolutional neural network. In *2017 IEEE International Conference on Bioinformatics and Biomedicine (BIBM)*, pages 1195–1200. IEEE, 2017.

[10] Nguyen P Nguyen, Tommi A White, and Filiz Bunyak. Mitochondria instance segmentation in electron microscopy image volumes using 3d deep learning networks. In *2021 IEEE Applied Imagery Pattern Recognition Workshop (AIPR)*, pages 1–6. IEEE, 2021.

[11] Ashish Pandey, Ramakrishna Surya, Matthew Maschmann, and Prasad Calyam. Reinforcement learning based carbon nanotube growth automation. In *2021 IEEE Applied Imagery Pattern Recognition Workshop (AIPR)*, pages 1–10. IEEE, 2021.

[12] Phuong Nguyen, Tarek Elgamal, Steven Konstanty, Todd Nicholson, Stuart Turner, Patrick Su, Klara Nahrstedt, Timothy Spila, Roy H Campbell, John Dallesasse, et al. Bracelet: Edge-cloud microservice infrastructure for aging scientific instruments. In *2019 International Conference on Computing, Networking and Communications (ICNC)*, pages 692–696. IEEE, 2019.

[13] Hengjing He, Wei Zhao, Songling Huang, Geoffrey C Fox, and Qing Wang. Research on the architecture and its implementation for instrumentation and measurement cloud. *IEEE Transactions on Services Computing*, 13(5):944–957, 2017.

[14] Matthew Dickinson, Saptarshi Debroy, Prasad Calyam, Samaikya Valluripally, Yuanxun Zhang, Ronny Bazan Antequera, Trupti Joshi, Tommi White, and Dong Xu. Multi-cloud performance and security driven federated workflow management. *IEEE Transactions on Cloud Computing*, 9(1):240–257, 2018.

[15] Phuong Nguyen, Steven Konstanty, Todd Nicholson, Thomas O'brien, Aaron Schwartz-Duval, Timothy Spila, Klara Nahrstedt, Roy H Campbell, Indranil Gupta, Michael Chan, et al. 4ceed: Real-time data acquisition and analysis framework for material-related cyber-physical environments. In *2017 17th IEEE/ACM International Symposium on Cluster, Cloud and Grid Computing (CCGRID)*, pages 11–20. IEEE, 2017.

[16] Jonathan Bouvette, Qinwen Huang, Alberto Bartesaghi, and Mario J Borgnia. Smartscope: Ai-driven grid navigation for high-throughput cryo-em. In *2021 IEEE Applied Imagery Pattern Recognition Workshop (AIPR)*, pages 1–6. IEEE, 2021.

[17] Boyuan Huang, Zhenghao Li, and Jiangyu Li. An artificial intelligence atomic force microscope enabled by machine learning. *Nanoscale*, 10(45):21320–21326, 2018.

[18] Giovanni Aloisi, Federico Bacci, Marcello Carlà, David Dolci, and Leonardo Lanzi. Implementation on a desktop computer of the real time feedback control loop of a scanning probe microscope. *Review of Scientific Instruments*, 79(11):113702, 2008.

[19] Soheil Aghajanian, Vesa Ruuskanen, Harri Nieminen, Arto Laari, Markus Honkanen, and Tuomas Koiranen. Real-time monitoring and insights into process control of micron-sized calcium carbonate crystallization by an in-line digital microscope camera. *Chemical Engineering Research and Design*, 177:778–788, 2022.

[20] Ákos Borsos, Botond Szilagyi, Paul Serban Agachi, and Zoltán K Nagy. Real-time image processing based online feedback control system for cooling batch crystallization. *Organic Process Research & Development*, 21(4):511–519, 2017.

[21] Matthew R Maschmann. Integrated simulation of active carbon nanotube forest growth and mechanical compression. *Carbon*, 86:26–37, 2015.
[22] Josef Brown, Taher Hajilounezhad, Nicholas T Dee, Sanha Kim, A John Hart, and Matthew R Maschmann. Delamination mechanics of carbon nanotube micropillars. *ACS applied materials & interfaces*, 11(38):35221–35227, 2019.
[23] Ryan Hines, Taher Hajilounezhad, Cole Love-Baker, Gordon Koerner, and Matthew R Maschmann. Growth and mechanics of heterogeneous, 3d carbon nanotube forest microstructures formed by sequential selective-area synthesis. *ACS Applied Materials & Interfaces*, 12(15):17893–17900, 2020.
[24] Janett Eckmann, Schamim H Eckert, Kristina Leuner, Walter E Muller, and Gunter P Eckert. Mitochondria: mitochondrial membranes in brain ageing and neurodegeneration. *The international journal of biochemistry & cell biology*, 45(1):76–80, 2013.
[25] Silvia Campello and Luca Scorrano. Mitochondrial shape changes: orchestrating cell pathophysiology. *EMBO Rep.*, 11(9):678–684, Sep 2010.
[26] Dong-Hyung Cho, Tomohiro Nakamura, and Stuart A. Lipton. Mitochondrial dynamics in cell death and neurodegeneration. *Cell. Mol. Life Sci.*, 67(20):3435–3447, Oct 2010.
[27] Michelle Barbi de Moura, Lucas Santana dos Santos, and Bennett Van Houten. Mitochondrial dysfunction in neurodegenerative diseases and cancer. *Environ. Mol. Mutagen.*, 51(5):391–405, Jun 2010.
[28] Aurélien Lucchi, Kevin Smith, Radhakrishna Achanta, Graham Knott, and Pascal Fua. Supervoxel-based segmentation of mitochondria in em image stacks with learned shape features. *IEEE transactions on medical imaging*, 31(2):474–486, 2011.
[29] Chi Xiao, Xi Chen, Weifu Li, Linlin Li, Lu Wang, Qiwei Xie, and Hua Han. Automatic mitochondria segmentation for em data using a 3d supervised convolutional network. *Frontiers in neuroanatomy*, 12:92, 2018.
[30] Daniel Franco-Barranco, Arrate Muñoz-Barrutia, and Ignacio Arganda-Carreras. Stable deep neural network architectures for mitochondria segmentation on electron microscopy volumes. *Neuroinformatics*, pages 1–14, 2021.
[31] Ilja Gubins, Marten L Chaillet, Gijs van der Schot, Remco C Veltkamp, Friedrich Förster, Yu Hao, Xiaohua Wan, Xuefeng Cui, Fa Zhang, Emmanuel Moebel, et al. Shrec 2020: Classification in cryo-electron tomograms. *Computers & Graphics*, 91:279–289, 2020.
[32] Hui Zhang, Jason E Fritts, and Sally A Goldman. Image segmentation evaluation: A survey of unsupervised methods. *Computer Vision and Image Understanding*, 110(2):260–280, 2008.
[33] Anna Lena Eberle, Richard Schalek, Jeff W Lichtman, Matt Malloy, Brad Thiel, and Dirk Zeidler. Multiple-beam scanning electron microscopy. *Microscopy Today*, 23(2):12–19, 2015.
[34] Diederik P. Kingma and Jimmy Ba. Adam: A method for stochastic optimization. In Yoshua Bengio and Yann LeCun, editors, *3rd International Conference on Learning Representations, ICLR 2015, San Diego, CA, USA, May 7-9, 2015, Conference Track Proceedings*, 2015.
[35] Donglai Wei, Zudi Lin, Daniel Franco-Barranco, Nils Wendt, Xingyu Liu, Wenjie Yin, Xin Huang, Aarush Gupta, Won-Dong Jang, Xueying Wang, Ignacio Arganda-Carreras, Jeff W. Lichtman, and Hanspeter Pfister. MitoEM Dataset: Large-scale 3D Mitochondria Instance Segmentation from EM Images. *Med. Image Comput. Comput. Assist. Interv.*, 12265:66–76, Oct 2020.